Proceedings of the Estonian Academy of Sciences,
2024, **73**, 1, 17–28
https://doi.org/10.3176/proc.2024.1.03
Available online at www.eap.ee/proceedings

DYNAMICAL SYSTEMS

Bifurcation analysis and optical soliton perturbation with Radhakrishnan–Kundu–Lakshmanan equation

Lu Tang[a], Anjan Biswas[b,c,d,e*], Yakup Yıldırım[f,g], Maggie Aphane[e] and Abdulah A. Alghamdi[c]

[a] School of Mathematics and Physics, Chengdu University of Technology, Chengdu 610059, China
[b] Department of Mathematics and Physics, Grambling State University, Grambling, LA 71245, USA
[c] Mathematical Modeling and Applied Computation (MMAC) Research Group, Department of Mathematics, King Abdulaziz University, Jeddah 21589, Saudi Arabia
[d] Department of Applied Sciences, Cross-Border Faculty of Humanities, Economics and Engineering, Dunarea de Jos University of Galati, 111 Domneasca Street, Galati 800201, Romania
[e] Department of Mathematics and Applied Mathematics, Sefako Makgatho Health Sciences University, Medunsa 0204, South Africa
[f] Department of Computer Engineering, Biruni University, Istanbul 34010, Turkey
[g] Department of Mathematics, Near East University, Nicosia 99138, Cyprus

Received 16 March 2023, accepted 11 April 2023, available online 21 December 2023

Abstract. This paper addresses Radhakrishnan–Kundu–Lakshmanan equation that arises in the study of soliton dynamics in optical fibers. The bifurcation analysis is carried out and the phase portraits are displayed. The complete discriminant analysis also leads to solitons and other solutions to the model.

Keywords: nonlinear Radhakrishnan–Kundu–Lakshmanan equation, bifurcation analysis, complete discriminant system, optical solitons.

1. INTRODUCTION

There are several models to address dispersive optical solitons. Some of them are Schrodinger–Hirota's equation, Fokas–Lenells equation, Lakshmanan–Porsezian–Daniel equation and many more. One of the lesser visible models is the Radhakrishnan–Kundu–Lakshmanan (RKL) equation that introduces a third-order dispersion (3OD) in addition to the pre-existing chromatic dispersion (CD). The nonlinear form of the refractive index stems from the effect of the Kerr law of nonlinearity. A wide range of results have been obtained with the RKL equation during the past few years since its introduction in 1999 [1–14]. The current paper is a revisitation of the RKL equation from a different perspective. The bifurcation analysis for this model will be addressed and the phase portrait analysis will be carried out in detail. Subsequently, the complete discrimination analysis will yield dark and singular solitons, singular periodic solutions as well as cnoidal waves. The surface plots of such solutions are also exhibited to gain a complete understanding of the model.

* Corresponding author, biswas.anjan@gmail.com

In the present work, we are going to consider the perturbed nonlinear RKL equation as follows [11,12]:

$$iu_t + b_1 u_{xx} + b_2|u|^2 u = i[\beta u_x + \mu(|u|^2 u)_x + \delta(|u|^2)_x u - \alpha u_{xxx}], \tag{1}$$

where $u = u(x,t)$ is the complex-valued function that represents the wave variable. x and t denote the spatial and temporal variables, respectively. The first term represents linear evolution, the coefficient b_1 stands for CD and b_2 represents the nonlinear term that is of Kerr type. On the right side of Eq. (1), nonzero constant β stands for the inter-modal dispersion that is considered in addition to CD. Furthermore, the coefficient μ is the self-steepening effect. δ stands for the effect of self-frequency shift. Finally, the coefficient α represents 3OD whenever group velocity dispersion (GVD) carries a low count. This work will retrieve some new dark solitons, singular solitons, bright solitons and some other traveling wave solutions by means of dynamical theory as well as the complete discriminant system technique.

The layout of this article is designed as follows. In Section 2, the corresponding phase diagrams and Hamiltonian function of system (1) have been obtained. Then, multiple optical soliton solutions are deduced by means of the dynamical theory. Some other traveling wave solutions are also recovered with the help of symbolic computation and the complete discriminant system method in Section 3. In Section 4, numerical simulations are given. Finally, we summarize the results of the current study in the last section.

2. PHASE PORTRAITS AND OPTICAL SOLITONS FOR THE PERTURBED RKL EQUATION

In order to analyze the dynamical behavior and seek the optical soliton solutions for the perturbed nonlinear RKL equation, we first assume that system (1) owns the traveling wave transformation as follows:

$$u(x,t) = P(\xi)\exp[i\eta(x,t)], \quad \xi = x - ct, \quad \eta(x,t) = -\lambda x + \kappa t + \omega_0, \tag{2}$$

where c represents the velocity, λ denotes the frequency, κ stands for the wave number and ω_0 denotes the phase constant.

On plugging (2) into (1) and separating the real and imaginary parts, we have

$$(b_1 + 3\alpha\lambda)P'' - (\kappa + \beta\lambda + b_1\lambda^2 + \alpha\lambda^3)P + (b_2 - \mu\lambda)P^3 = 0 \tag{3}$$

and

$$3\alpha P'' - 3(c + \beta + 2b_1\lambda + 3\alpha\lambda^2)P - (3\mu + 2\delta)P^3 = 0. \tag{4}$$

For Eq. (3), note that $P' = \phi$, then we can easily obtain a planar dynamical system

$$\begin{cases} \frac{dP}{d\xi} = \phi, \\ \frac{d\phi}{d\xi} = -C_1 P^3 + C_2 P, \end{cases} \tag{5}$$

with the Hamiltonian

$$H(P,\phi) = \frac{1}{2}\phi^2 + \frac{C_1}{4}P^4 - \frac{C_2}{2}P^2 = h, \tag{6}$$

where $C_1 = \frac{b_2 - \mu\lambda}{b_1 + 3\alpha\lambda}$ and $C_2 = \frac{\kappa + \beta\lambda + b_1\lambda^2 + \alpha\lambda^3}{b_1 + 3\alpha\lambda}$.

Next, in order to obtain the plane phase portraits of system (5), note that $F(P) = -C_1P^3 + C_2P$. If $C_1C_2 > 0$, we can easily observe three zeros of $F(P)$, which include $P_0 = 0$, $P_1 = -\sqrt{\frac{C_2}{C_1}}$ and $P_2 = \sqrt{\frac{C_2}{C_1}}$. If $C_1C_2 < 0$, we get one zero of $F(P)$, which is $P_3 = 0$. Suppose that $M_i(P_i, 0)$ $(i = 0, 1, 2)$ are the equilibrium points of

system (5), then the eigenvalue of system (5) at the equilibrium point is written as $\lambda_{1,2} = \pm\sqrt{F'(P)}$. According to the qualitative theory of planar dynamical systems [15,16], it is easy to notice that the equilibrium point $M_i(P_i,0)$ is called a saddle point when $F'(P_i) > 0$, the equilibrium point $M_i(P_i,0)$ is called a degraded saddle point when $F'(P_i) = 0$, the equilibrium point $M_i(P_i,0)$ is called a center point when $F'(P_i) < 0$. Depending on different parameters C_1 and C_2, the phase portraits of system (5) are shown in Figs 1 and 2.

Case 1.1. $C_1 > 0, C_2 > 0$

In this case, we observe that system (5) owns three equilibrium points. $M_1(-\sqrt{\frac{C_2}{C_1}},0)$ and $M_2(\sqrt{\frac{C_2}{C_1}},0)$ are center points, $M_0(0,0)$ is a saddle point (see Fig. 2).

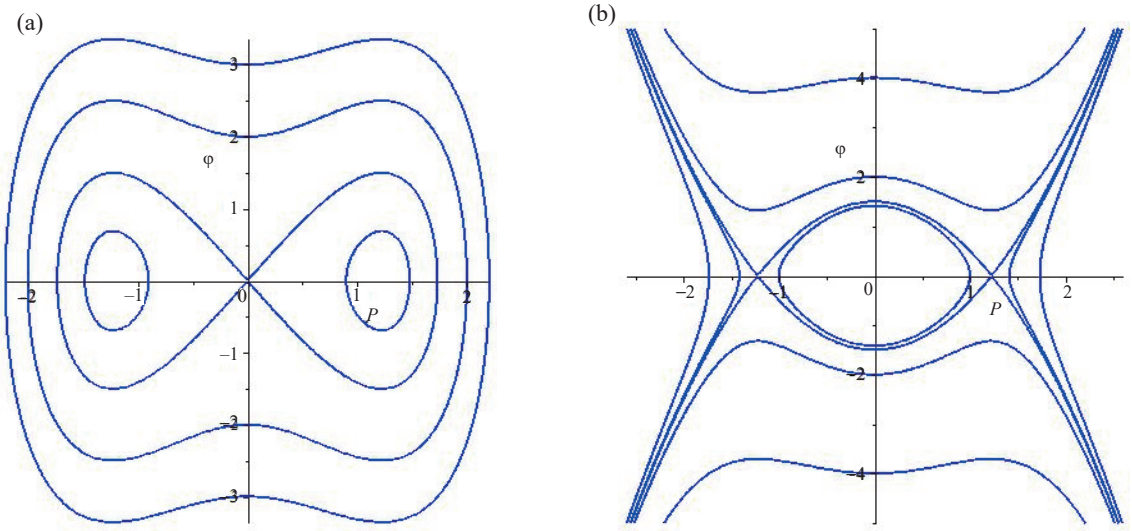

$C_1 > 0, C_2 > 0$ $C_1 < 0, C_2 < 0$

Fig. 1. The bifurcation phase portraits of system (5).

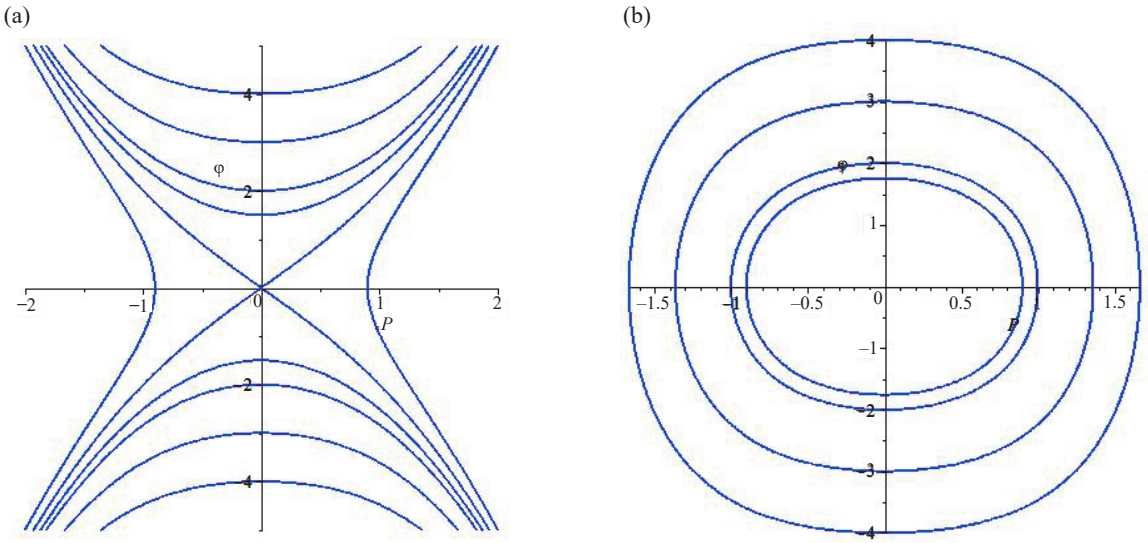

$C_1 < 0, C_2 > 0$ $C_1 > 0, C_2 < 0$

Fig. 2. The bifurcation phase portraits of system (5).

(i) When $h \in (-\frac{C_2^2}{4C_1}, 0)$, we observe that there exist two families of periodic orbits, then Eq. (6) can be modified as follows:

$$\phi^2 = \frac{C_1}{2}(-P^4 + \frac{2C_2}{C_1}P^2 + \frac{4h}{C_1}) = \frac{C_1}{2}(P^2 - z_1^2)(z_2^2 - P^2), \tag{7}$$

where $z_1^2 = \frac{C_2}{C_1} - \frac{1}{C_1}\sqrt{C_2^2 + 4C_1h}$ and $z_2^2 = \frac{C_2}{C_1} + \frac{1}{C_1}\sqrt{C_2^2 + 4C_1h}$. Next, by using (7) to integrate the first equation of (5) along the periodic orbits, we get the two integral equations in the following forms:

$$\int_P^{z_2} \frac{d\varphi}{\sqrt{(\varphi^2 - z_1^2)(z_2^2 - \varphi^2)}} = \pm\sqrt{\frac{C_1}{2}}(\xi - \xi_0) \tag{8}$$

and

$$\int_{-z_2}^{P} \frac{d\varphi}{\sqrt{(\varphi^2 - z_1^2)(z_2^2 - \varphi^2)}} = \pm\sqrt{\frac{C_1}{2}}(\xi - \xi_0). \tag{9}$$

Thus, we construct the smooth periodic solution of system (1) in the following form:

$$u_{1,1}(x,t) = \pm z_2 dn\left(z_2\sqrt{\frac{C_1}{2}}(x - ct - \xi_0), \frac{\sqrt{z_2^2 - z_1^2}}{z_2}\right) \times \exp(i(-\lambda x + \kappa t + \omega_0)). \tag{10}$$

It is obvious to find that $u_{1,1}$ stands for the Jacobian elliptic function solution. As is shown in Fig. 2, we observe that $u_{1,1}(x,t)$ denotes two families of periodic orbits in the right half-plane and left half-plane.

(ii) For $h = 0$, we get $z_1^2 = 0$ and $z_2^2 = \frac{2C_2}{C_1}$. Therefore, the two bell-shaped solitary wave solutions of system (1) take the form

$$u_{1,2}(x,t) = \pm\sqrt{\frac{2C_2}{C_1}} sech\left(\sqrt{C_2}(x - ct - \xi_0)\right) \times \exp(i(-\lambda x + \kappa t + \omega_0)). \tag{11}$$

(iii) When $h \in (0, +\infty)$, one has

$$\phi^2 = \frac{C_1}{2}(-P^4 + \frac{2C_2}{C_1}P^2 + \frac{4h}{C_1}) = \frac{C_1}{2}(P^2 + z_{1h}^2)(z_{2h}^2 - P^2), \tag{12}$$

where $z_{1h}^2 = -\frac{C_2}{C_1} + \frac{1}{C_1}\sqrt{C_2^2 + 4C_1h}$ and $z_{2h}^2 = \frac{C_2}{C_1} + \frac{1}{C_1}\sqrt{C_2^2 + 4C_1h}$.

Inserting (12) into the first equation of (5), integrating them along the periodic orbits, we have

$$\int_0^P \frac{d\varphi}{\sqrt{(\varphi^2 + z_{1h}^2)(z_{2h}^2 - \varphi^2)}} = \pm\sqrt{\frac{C_1}{2}}(\xi - \xi_0), \tag{13}$$

where ξ_0 is the integral constant. From (2) and (13), the periodic traveling wave solutions of system (1) are as follows:

$$u_{1,3}(x,t) = \pm z_{2h} cn\left(\sqrt{\frac{C_1(z_{1h}^2 + z_{2h}^2)}{2}}(x - ct - \xi_0), \frac{z_{2h}}{\sqrt{z_{1h}^2 + z_{2h}^2}}\right) \times \exp(i(-\lambda x + \kappa t + \omega_0)). \tag{14}$$

Case 1.2. $C_1 < 0, C_2 < 0$

Under the conditions of $C_1 < 0$ and $C_2 < 0$, we find that there are two heteroclinic orbits of system (5), which connect two saddle points $M_1 = (-\sqrt{\frac{C_2}{C_1}}, 0)$ and $M_2 = (\sqrt{\frac{C_2}{C_1}}, 0)$. As is shown in Fig. 1, there is a family of periodic orbits, which enclose the center point $M_0(0,0)$.

(i) When $h \in (0, -\frac{C_2^2}{4C_1})$, we notice that there exists a family of periodic orbits of (5) defined by the following algebraic equation:

$$\phi^2 = -\frac{C_1}{2}(P^4 + \frac{2C_2}{C_1}P^2 - \frac{4h}{C_1}) = -\frac{C_1}{2}(z_{3h}^2 - P^2)(z_{4h}^2 - P^2), \tag{15}$$

where $z_{3h}^2 = \frac{C_2}{C_1} - \frac{1}{C_1}\sqrt{C_2^2 + 4C_1 h}$ and $z_{4h}^2 = \frac{C_2}{C_1} + \frac{1}{C_1}\sqrt{C_2^2 + 4C_1 h}$.

Plugging (15) into the first equation of (5), then integrating them along the periodic orbits, we get

$$\int_0^P \frac{d\varphi}{\sqrt{(z_{3h}^2 - \varphi^2)(z_{4h}^2 - \varphi^2)}} = \pm\sqrt{-\frac{C_1}{2}}(\xi - \xi_0). \tag{16}$$

According to (2) and (16), we construct the traveling wave solutions of system (1) in the following form:

$$u_{1,4}(x,t) = \pm z_{3h} sn\left(z_{4h}\sqrt{-\frac{C_1}{2}}(x - ct - \xi_0), \frac{z_{3h}}{z_{4h}}\right) \times \exp(i(-\lambda x + \kappa t + \omega_0)). \tag{17}$$

(ii) When $h = -\frac{C_2^2}{4C_1}$, we derive that $z_{3h}^2 = z_{4h}^2 = \frac{C_2}{C_1}$. As a consequence, we deduce two families of kink-shaped solitary wave solutions of (1) in the following form:

$$u_{1,5}(x,t) = \pm\sqrt{\frac{C_2}{C_1}}\tanh\left(\sqrt{-\frac{C_2}{2}}(x - ct - \xi_0)\right) \times \exp(i(-\lambda x + \kappa t + \omega_0)). \tag{18}$$

3. TRAVELING WAVE SOLUTIONS FOR THE RKL EQUATION VIA THE COMPLETE DISCRIMINANT SYSTEM METHOD

It is generally known that professor Yang and his team [17] introduced an algorithm in 1996, which could calculate the complete discrimination system of higher-order polynomials with the help of the computer algebra. In recent years, many researchers and scholars have constructed many different types of solitary wave solutions [18–25] through the complete discriminant system technique.

Next, we take (3) into consideration by multiplying it with P', and integrating once, we have

$$(P')^2 = E_4 P^4 + E_2 P^2 + E_0, \tag{19}$$

where $E_4 = -\frac{b_2 - \mu\lambda}{2b_1 + 6\alpha\lambda}$, $E_2 = \frac{\kappa + \beta\lambda + b_1\lambda^2 + \alpha\lambda^3}{b_1 + 3\alpha\lambda}$ and E_0 is the integration constant.

Consider the following transformation:

$$\begin{cases} P = \pm\sqrt{(4E_4)^{-\frac{1}{3}}\Phi}, \\ e_1 = 4E_2(4E_4)^{-\frac{2}{3}}, \\ e_0 = 4E_0(4E_4)^{-\frac{1}{3}}, \\ \xi_1 = (4E_4)^{\frac{1}{3}}\xi. \end{cases} \tag{20}$$

Then Eq. (20) can be modified as follows:

$$(\frac{d\Phi}{d\xi_1})^2 = \Phi(\Phi^2 + e_1\Phi + e_0). \tag{21}$$

Integrating (21) once, we deduce

$$\int \frac{d\Phi}{\sqrt{\Phi(\Phi^2 + e_1\Phi + e_0)}} = \pm(\xi_1 - \xi_0), \tag{22}$$

where ξ_0 is the integration constant and denotes the value of ξ_0 as zero. Let $G(\Phi) = \Phi^2 + e_1\Phi + e_0$; therefore, we derive its complete discrimination system as follows:

$$\Delta = e_1^2 - 4e_0. \tag{23}$$

It follows from the root-classifications of (23) that there are four cases to be discussed.

Case 2.1. Assume that $\Delta = 0$. As for $\Phi > 0$, we get

$$\pm(\xi_1 - \xi_0) = \int \frac{d\Phi}{\sqrt{\Phi}(\Phi + \frac{e_1}{2})}. \tag{24}$$

When $e_1 > 0$, it follows from (2), (20) and (24) that the optical soliton solutions of (1) take the form

$$\begin{aligned} u_{2,1}(x,t) &= \pm\sqrt{\frac{\kappa + \beta\lambda + b_1\lambda^2 + \alpha\lambda^3}{\mu\lambda - b_2}} \times \exp(i(-\lambda x + \kappa t + \omega_0)) \\ &\times \tan\left\{2^{-\frac{7}{6}}\sqrt{\frac{\kappa + \beta\lambda + b_1\lambda^2 + \alpha\lambda^3}{b_1 + 3\alpha\lambda}}(\frac{2b_1 + 6\alpha\lambda}{\mu\lambda - b_2})^{\frac{1}{3}}\left[(\frac{2\mu\lambda - 2b_2}{b_1 + 3\alpha\lambda})^{\frac{1}{3}}\xi - \xi_0\right]\right\}. \end{aligned} \tag{25}$$

If $e_1 < 0$, from (2), (20) and (24), system (1) owns the traveling wave solutions as follows:

$$\begin{aligned} u_{2,2}(x,t) &= \pm\sqrt{-\frac{\kappa + \beta\lambda + b_1\lambda^2 + \alpha\lambda^3}{\mu\lambda - b_2}} \times \exp(i(-\lambda x + \kappa t + \omega_0)) \\ &\times \tanh\left\{2^{-\frac{7}{6}}\sqrt{-\frac{\kappa + \beta\lambda + b_1\lambda^2 + \alpha\lambda^3}{b_1 + 3\alpha\lambda}}(\frac{2b_1 + 6\alpha\lambda}{\mu\lambda - b_2})^{\frac{1}{3}}\left[(\frac{2\mu\lambda - 2b_2}{b_1 + 3\alpha\lambda})^{\frac{1}{3}}\xi - \xi_0\right]\right\} \end{aligned} \tag{26}$$

and

$$\begin{aligned} u_{2,3}(x,t) &= \pm\sqrt{-\frac{\kappa + \beta\lambda + b_1\lambda^2 + \alpha\lambda^3}{\mu\lambda - b_2}} \times \exp(i(-\lambda x + \kappa t + \omega_0)) \\ &\times \coth\left\{2^{-\frac{7}{6}}\sqrt{-\frac{\kappa + \beta\lambda + b_1\lambda^2 + \alpha\lambda^3}{b_1 + 3\alpha\lambda}}(\frac{2b_1 + 6\alpha\lambda}{\mu\lambda - b_2})^{\frac{1}{3}}\left[(\frac{2\mu\lambda - 2b_2}{b_1 + 3\alpha\lambda})^{\frac{1}{3}}\xi - \xi_0\right]\right\}. \end{aligned} \tag{27}$$

When $e_1 = 0$, the rational function solutions of system (1) are as follows:

$$u_{2,4}(x,t) = \pm 2^{\frac{2}{3}}(-\frac{b_2 - \mu\lambda}{2b_1 + 6\alpha\lambda})^{-\frac{1}{6}} \times \exp(i(-\lambda x + \kappa t + \omega_0)) \times [(\frac{2\mu\lambda - 2b_2}{b_1 + 3\alpha\lambda})^{\frac{1}{3}}\xi - \xi_0]^{-1}. \tag{28}$$

Case 2.2. Assume that $\Delta > 0$ and $e_0 = 0$. As for $\Phi > -e_1$, we have

$$\pm(\xi_1 - \xi_0) = \int \frac{d\Phi}{\Phi\sqrt{\Phi + e_1}}. \tag{29}$$

If $e_1 > 0$, it follows from (2), (20) and (29) that the optical soliton solutions of system (1) can be deduced as follows:

$$\begin{aligned} u_{2,5}(x,t) &= \pm\sqrt{\frac{\kappa+\beta\lambda+b_1\lambda^2+\alpha\lambda^3}{\mu\lambda-b_2}} \times \exp(i(-\lambda x+\kappa t+\omega_0)) \\ &\times \left\{ \tanh^2 \left[2^{-\frac{7}{6}} \sqrt{\frac{\kappa+\beta\lambda+b_1\lambda^2+\alpha\lambda^3}{b_1+3\alpha\lambda}} (\frac{2b_1+6\alpha\lambda}{\mu\lambda-b_2})^{\frac{1}{3}} \left[(\frac{2\mu\lambda-2b_2}{b_1+3\alpha\lambda})^{\frac{1}{3}} \xi - \xi_0 \right] \right] - 2 \right\}^{\frac{1}{2}} \end{aligned} \tag{30}$$

and

$$\begin{aligned} u_{2,6}(x,t) &= \pm\sqrt{\frac{\kappa+\beta\lambda+b_1\lambda^2+\alpha\lambda^3}{\mu\lambda-b_2}} \times \exp(i(-\lambda x+\kappa t+\omega_0)) \\ &\times \left\{ \coth^2 \left[2^{-\frac{7}{6}} \sqrt{\frac{\kappa+\beta\lambda+b_1\lambda^2+\alpha\lambda^3}{b_1+3\alpha\lambda}} (\frac{2b_1+6\alpha\lambda}{\mu\lambda-b_2})^{\frac{1}{3}} \left[(\frac{2\mu\lambda-2b_2}{b_1+3\alpha\lambda})^{\frac{1}{3}} \xi - \xi_0 \right] \right] - 2 \right\}^{\frac{1}{2}}. \end{aligned} \tag{31}$$

When $e_1 < 0$, from (2), (20) and (29), the optical soliton solutions of system (1) can be constructed in the following form:

$$\begin{aligned} u_{2,7}(x,t) &= \pm\sqrt{-\frac{\kappa+\beta\lambda+b_1\lambda^2+\alpha\lambda^3}{\mu\lambda-b_2}} \times \exp(i(-\lambda x+\kappa t+\omega_0)) \\ &\times \left\{ \tan^2 \left[2^{-\frac{7}{6}} \sqrt{-\frac{\kappa+\beta\lambda+b_1\lambda^2+\alpha\lambda^3}{b_1+3\alpha\lambda}} (\frac{2b_1+6\alpha\lambda}{\mu\lambda-b_2})^{\frac{1}{3}} \left[(\frac{2\mu\lambda-2b_2}{b_1+3\alpha\lambda})^{\frac{1}{3}} \xi - \xi_0 \right] \right] + 2 \right\}^{\frac{1}{2}}. \end{aligned} \tag{32}$$

Case 2.3. Assume that $\Delta > 0$, $e_0 \neq 0$ and $\gamma_1 < \gamma_2 < \gamma_3$, and then we suppose that one of γ_1, γ_2, γ_3 is zero and the rest of them are two different roots of $G(\Phi) = 0$. By considering the following transformation $\Phi = \gamma_1 + (\gamma_2 - \gamma_1)\sin^2\theta$, we obtain

$$\pm(\xi_1 - \xi_0) = \frac{2}{\sqrt{\gamma_3 - \gamma_1}} \int \frac{d\theta}{\sqrt{1 - k_1^2 \sin^2\theta}}, \tag{33}$$

where $k_1^2 = \frac{\gamma_2 - \gamma_1}{\gamma_3 - \gamma_1}$. From (2), (20) and (33), we deduce the Jacobian elliptic function solutions of (1) in the following form:

$$\begin{aligned} u_{2,8}(x,t) &= \pm(\frac{2\mu\lambda-2b_2}{b_1+3\alpha\lambda})^{-\frac{1}{6}} \times \exp(i(-\lambda x+\kappa t+\omega_0)) \\ &\times \left\{ \gamma_1 + (\gamma_2-\gamma_1) sn^2 \left(\frac{\sqrt{\gamma_3-\gamma_1}}{2} [(\frac{2\mu\lambda-2b_2}{b_1+3\alpha\lambda})^{\frac{1}{3}} \xi - \xi_0], k_1 \right) \right\}^{\frac{1}{2}}. \end{aligned} \tag{34}$$

For another transformation $\Phi = \frac{-\gamma_2 \sin^2\theta+\gamma_3}{\cos^2\theta}$, from (2), (20) and (33), we construct the Jacobian elliptic function solutions of system (1):

$$u_{2,9}(x,t) = \pm\left(\frac{2\mu\lambda - 2b_2}{b_1+3\alpha\lambda}\right)^{-\frac{1}{6}} \times \exp(i(-\lambda x+\kappa t+\omega_0)) \times \left\{ \frac{-\gamma_2 sn^2\left(\frac{\sqrt{\gamma_3-\gamma_1}}{2}\left[\left(\frac{2\mu\lambda-2b_2}{b_1+3\alpha\lambda}\right)^{\frac{1}{3}}\xi-\xi_0\right],k_1\right)+\gamma_3}{cn^2\left(\frac{\sqrt{\gamma_3-\gamma_1}}{2}\left[\left(\frac{2\mu\lambda-2b_2}{b_1+3\alpha\lambda}\right)^{\frac{1}{3}}\xi-\xi_0\right],k_1\right)} \right\}^{\frac{1}{2}}. \tag{35}$$

Case 2.4. Assume that $\Delta < 0$. By using the transformation $\Phi = \sqrt{e_0}\tan^2\frac{\theta}{2}$, we derive

$$\pm(\xi_1-\xi_0) = (e_0)^{-\frac{1}{4}} \int \frac{d\theta}{1-k_2^2\sin^2\theta}, \tag{36}$$

where $k_2^2 = \frac{2\sqrt{e_0}-e_1}{4\sqrt{e_0}}$. According to (2), (20) and (36), we derive the Jacobian elliptic function solutions of system (1) as follows:

$$u_{2,10}(x,t) = \pm\left(\frac{2b_1E_0+6\alpha\lambda E_0}{\mu\lambda-b_2}\right)^{\frac{1}{4}} \times \exp(i(-\lambda x+\kappa t+\omega_0)) \times \left\{ \frac{2}{1+cn\left[\left(\frac{32b_1A_0^3+96\alpha\lambda A_0^3}{\mu\lambda-b_2}\right)^{\frac{1}{12}}\left[\left(\frac{2\mu\lambda-2b_2}{b_1+3\alpha\lambda}\right)^{\frac{1}{3}}\xi-\xi_0\right],k_2\right]} - 1 \right\}^{\frac{1}{2}}. \tag{37}$$

4. NUMERICAL SIMULATIONS

In this section, we are going to select some suitable parameters to simulate traveling wave solutions of system (1) in a two-dimensional and three-dimensional space. As is shown in the graphs, we find that Fig. 3a stands for the bright soliton solutions $u_{1,2}$, Fig. 5a signifies the envelope of the dark soliton solutions $u_{1,5}$ and Fig. 7a denotes the rational function solutions $u_{2,4}$. Also, two-dimensional plots (Figs 3b, 5b, 7b) stand for the level curve at two different times $t = 1$ and $t = 0$. Figures 4a, 6a, 8a and Figs 4b, 6b, 8b represent the density and contour plots.

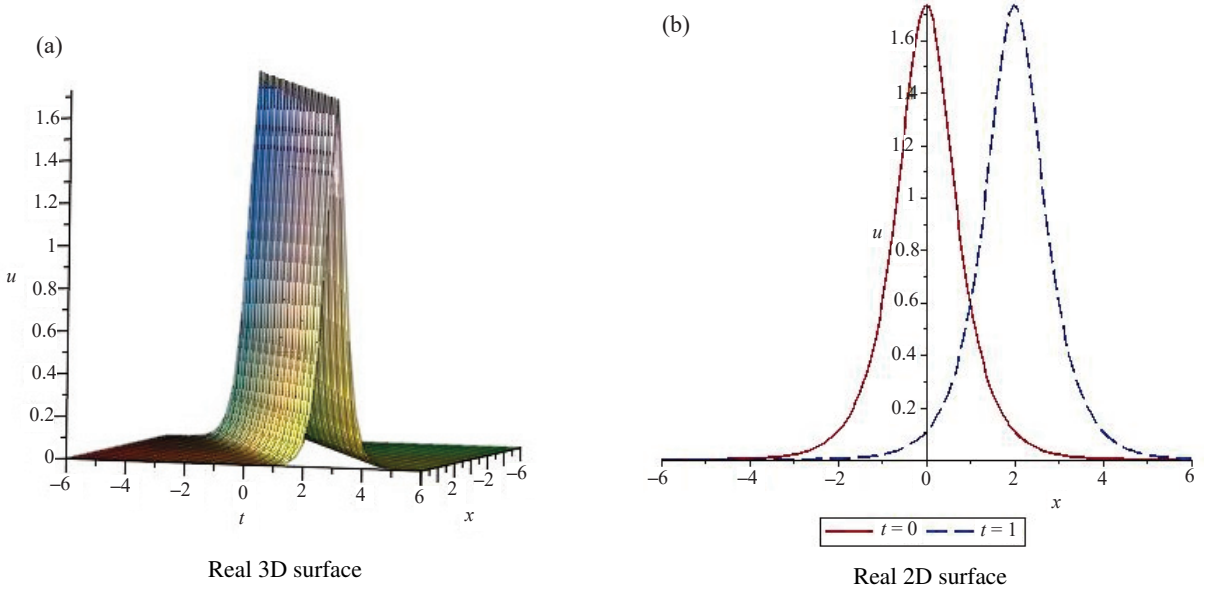

Real 3D surface

Real 2D surface

Fig. 3. The diagrams of $u_{1,2}(x,t)$ in Eq. (11) at $C_1 = 2, C_2 = 3, A = 1, c = 2, \xi_0 = 0$.

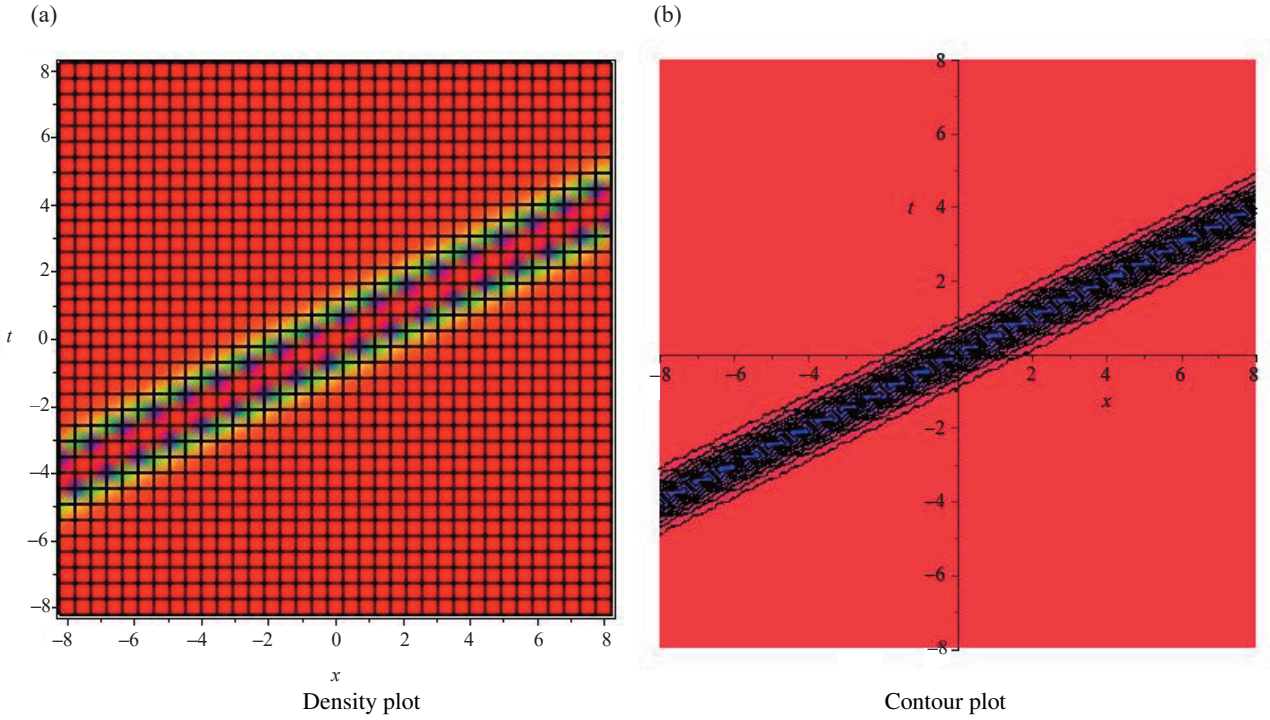

Fig. 4. The diagrams of $u_{1,2}(x,t)$ in Eq. (11) at $C_1 = 2$, $C_2 = 3$, $c = 2$, $\xi_0 = 0$.

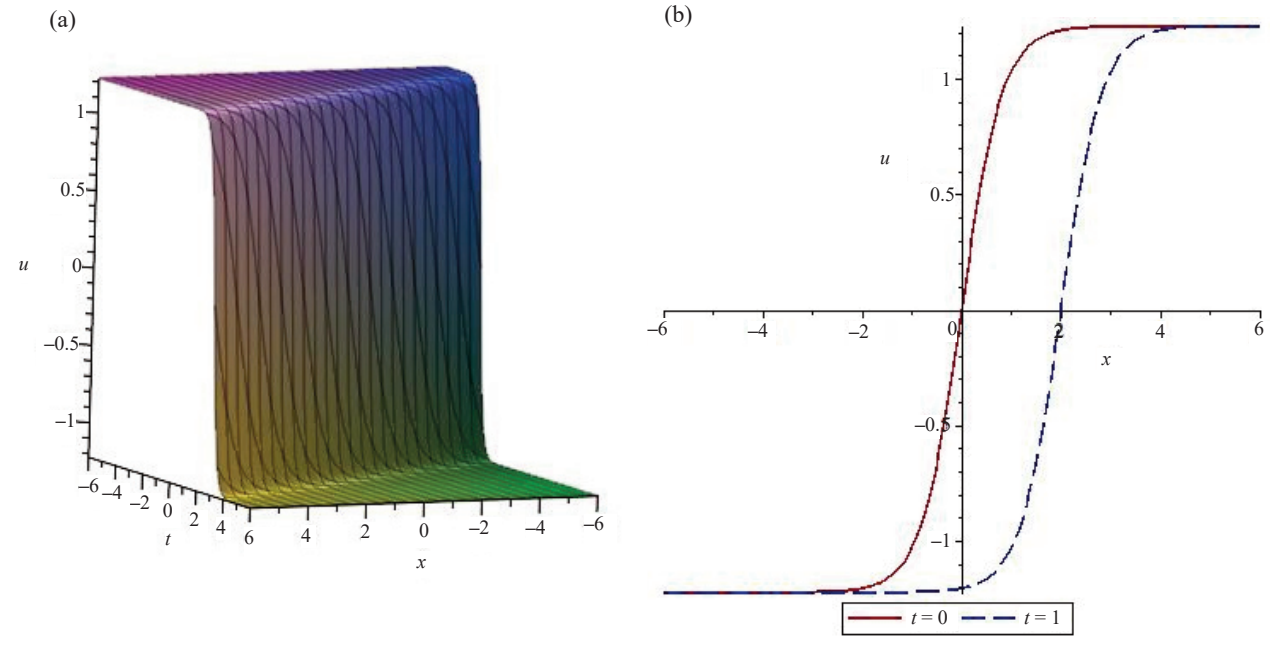

Fig. 5. The diagrams of $u_{1,5}(x,t)$ in Eq. (18) at $C_1 = -2$, $C_2 = -3$, $c = 2$, $\xi_0 = 0$.

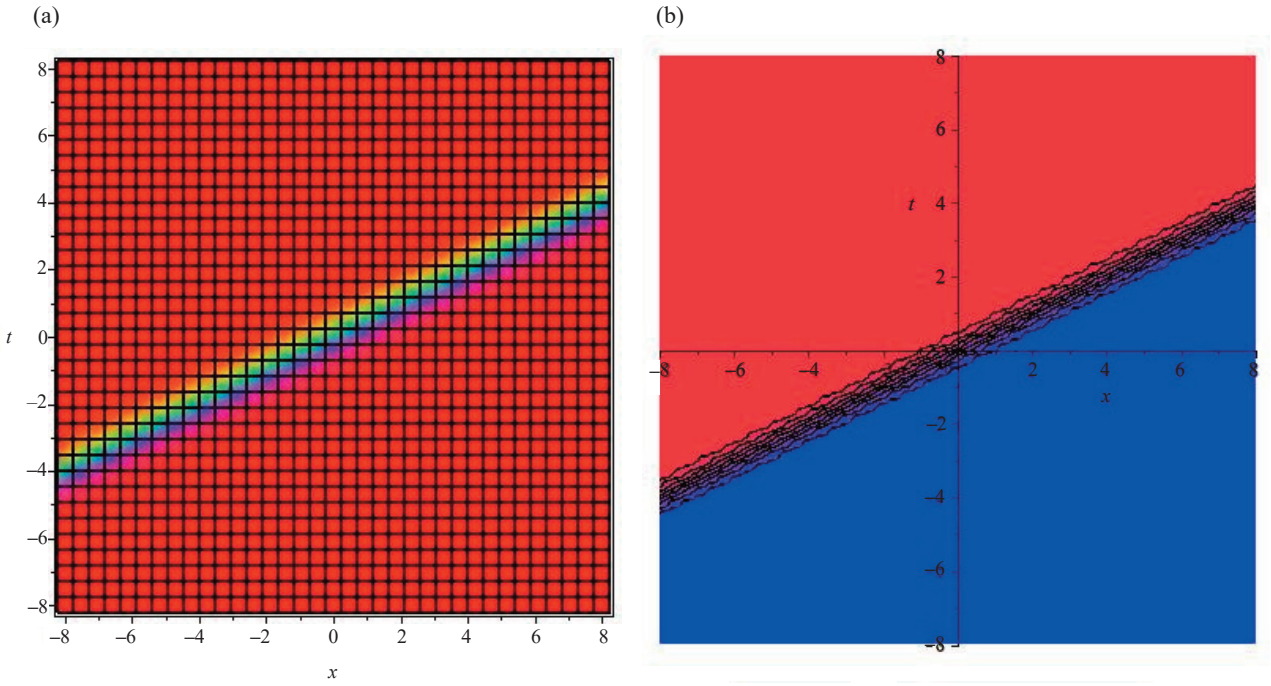

Fig. 6. The diagrams of $u_{1,5}(x,t)$ in Eq. (18) at $C_1 = -2$, $C_2 = -3$, $c = 2$, $\xi_0 = 0$.

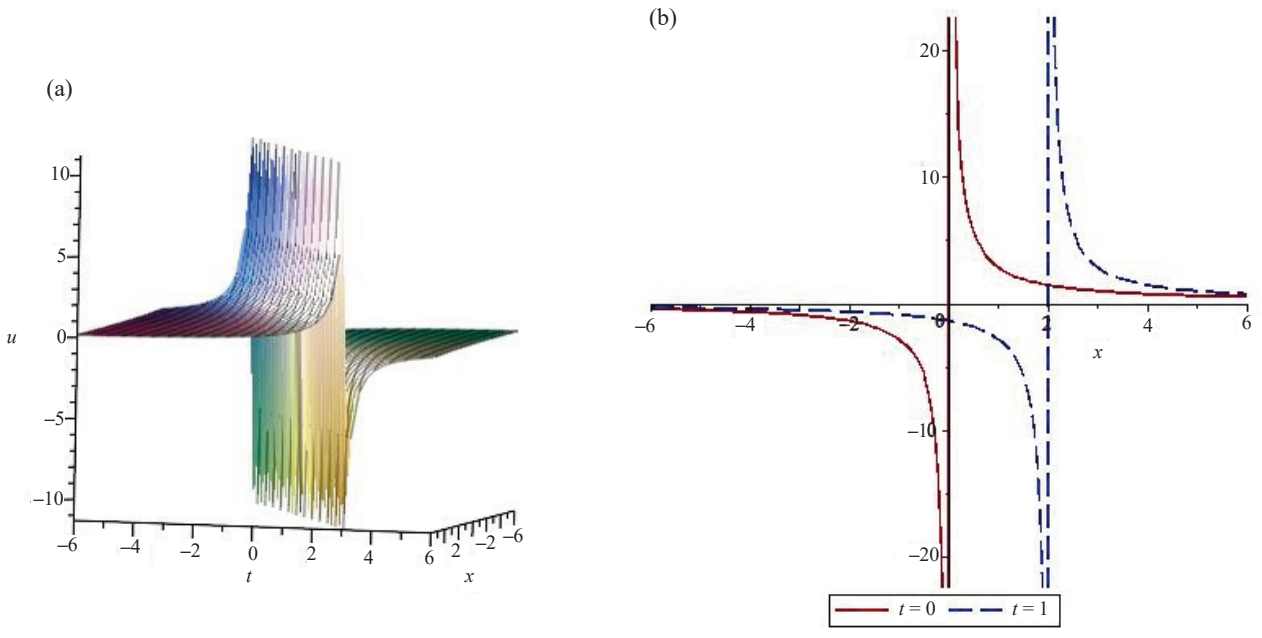

Fig. 7. The diagrams of $u_{2,4}(x,t)$ in Eq. (28) at $b_1 = b_2 = \alpha = \lambda = 1$, $\mu = 2$, $c = 2$, $\xi_0 = 0$.

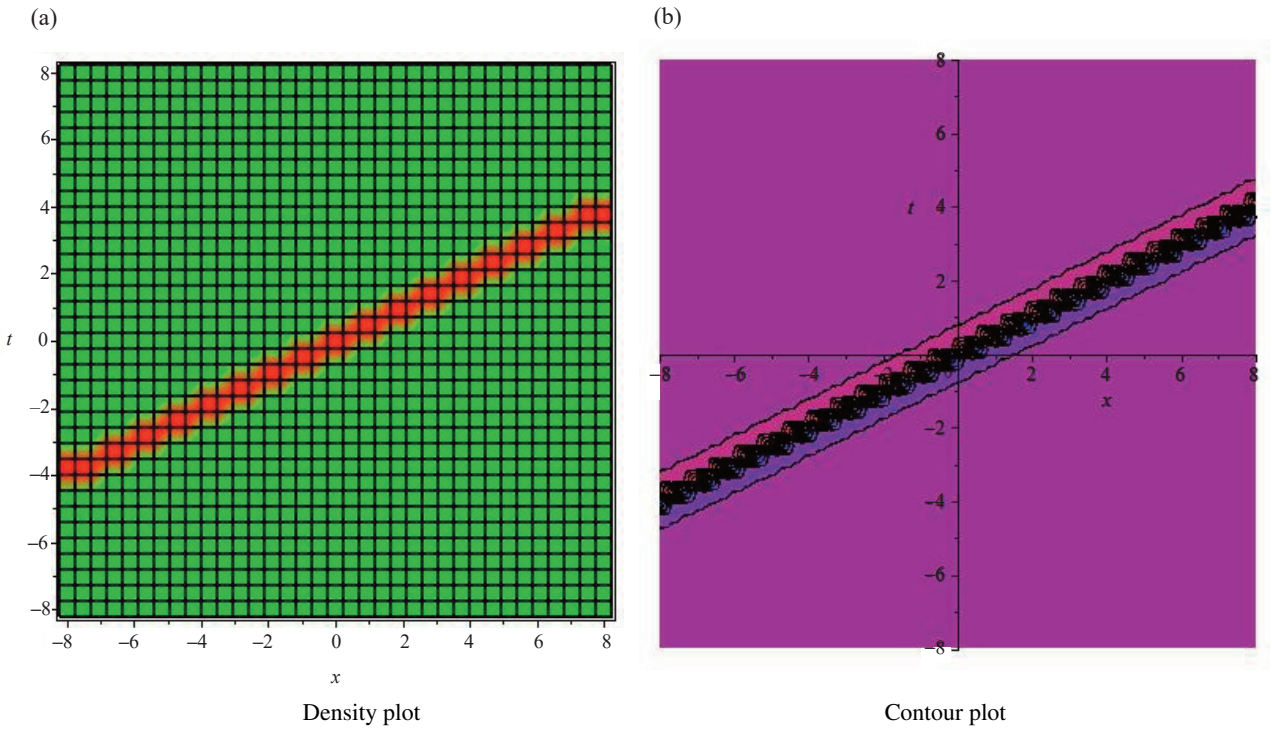

Fig. 8. The diagrams of $u_{2,4}(x,t)$ in Eq. (28) at $b_1 = b_2 = \alpha = \lambda = 1$, $\mu = 2$, $c = 2$, $\xi_0 = 0$.

5. CONCLUSIONS

The current paper is a complete understanding of the RKL equation from the bifurcation point of view. The dynamical system of the parameters gave way to the analysis and the evolution of the phase portraits. The complete discrimination system analysis also yielded solitons, cnoidal waves and singular periodic solutions to the model. This novel analysis for the RKL model is reported for the first time in the work. The results are extremely promising. Later, the analysis will be further carried out with additional forms of the nonlinear refractive index for the RKL model. Some preliminary results for such models have already been reported in those cases. The bifurcation analysis is yet to be carried out and those results are currently awaited.

ACKNOWLEDGMENT

The publication costs of this article were partially covered by the Estonian Academy of Sciences.

REFERENCES

1. Radhakrishnan, R., Kundu, A. and Lakshmanan, M. Coupled nonlinear Schrödinger equations with cubic–quintic nonlinearity: integrability and soliton interaction in non-Kerr media. *Phys. Rev. E*, 1999, **60**, 3314.
2. Garai, S. and Ghose-Choudhury, A. On the solution of the generalized Radhakrishnan–Kundu–Lakshmanan equation. *Optik*, 2021, **243**, 167374.
3. Huang, C. and Li, Z. Soliton solutions of conformable time-fractional perturbed Radhakrishnan–Kundu–Lakshmanan equation. *AIMS Mathematics*, 2022, **7**(8), 14460–14473.
4. Kudryashov, N. A., Safonova, D. V. and Biswas, A. Painlevé analysis and a solution to the traveling wave reduction of the Radhakrishnan–Kundu–Lakshmanan Equation. *Regul. Chaotic Dyn.*, 2019, **24**, 607–614.
5. Kudryashov, N. A. The Radhakrishnan–Kundu–Lakshmanan equation with arbitrary refractive index and its exact solutions. *Optik*, 2021, **238**, 166738.

6. Kudryashov, N. A. Revised results of Khalida Bibi on the Radhakrishnan–Kundu–Lakshmanan equation. *Optik*, 2021, **240**, 166898.
7. Kudryashov, N. A. Solitary waves of the generalized Radhakrishnan–Kundu–Lakshmanan equation with four powers of nonlinearity. *Phys. Lett. A*, 2022, **448**, 128327.
8. Ozdemir, N. Optical solitons for Radhakrishnan–Kundu–Lakshmanan equation in the presence of perturbation term and having Kerr law. *Optik*, 2022, **271**, 170127.
9. Ozdemir, N., Esen, H., Secer, A., Bayram, M., Sulaiman, T. A., Yusuf, A. et al. Optical solitons and other solutions to the Radhakrishnan–Kundu–Lakshmanan equation. *Optik*, 2021, **242**, 167363.
10. Wang, K.-J. and Si, J. Optical solitons to the Radhakrishnan–Kundu–Lakshmanan equation by two effective approaches. *Eur. Phys. J. Plus*, 2022, **137**, 1016.
11. Biswas, A. Optical soliton perturbation with Radhakrishnan–Kundu–Lakshmanan equation by traveling wave hypothesis. *Optik*, 2018, **171**, 217–220.
12. Bansal, A., Biswas, A., Mahmood, M. F., Zhou, Q., Mirzazadeh, M., Alshomrani, A. S. et al. Optical soliton perturbation with Radhakrishnan–Kundu–Lakshmanan equation by Lie group analysis. *Optik*, 2018, **163**, 137–141.
13. Wazwaz, A.-M. Painlevé integrability and lump solutions for two extended (3 + 1)- and (2 + 1)-dimensional Kadomtsev–Petviashvili equations. *Nonlinear Dyn.*, 2022, **111**, 3623–3632.
14. Wazwaz, A.-M., Hammad, M. A. and El-Tantawy, S. A. Bright and dark optical solitons for (3 + 1)-dimensional hyperbolic nonlinear Schrödinger equation using a variety of distinct schemes. *Optik*, 2022, **270**, 170043.
15. Li, J. and Dai, H. On the study of singular nonlinear traveling wave equations: dynamical system approach. *Science Press, Beijing*, 2007.
16. Li, J. B. Singular nonlinear traveling wave equations: bifurcation and exact solutions. *Science Press, Beijing*, 2013.
17. Yang, L., Hou, X. R., Zeng, Z. Complete discrimination system for polynomials. *Sci. China Ser. E*, 1996, **39**(6), 628–646.
18. Tang, L. Bifurcation analysis and multiple solitons in birefringent fibers with coupled Schrödinger–Hirota equation. *Chaos Solitons Fractals*, 2022, **161**, 112383.
19. Tang, L. Bifurcations and multiple optical solitons for the dual-mode nonlinear Schrödinger equation with Kerr law nonlinearity. *Optik*, 2022, **265**, 169555.
20. Xie, Y., Yang, Z. and Li, L. New exact solutions to the high dispersive cubic–quintic nonlinear Schrödinger equation. *Phys. Lett. A*, 2018, **382**(36), 2506–2514.
21. Tang, L. Bifurcations and dispersive optical solitons for the nonlinear Schrödinger–Hirota equation in DWDM networks. *Optik*, 2022, **262**, 169276.
22. Tang, L. Bifurcations and disperive optical solitons for the cubic–quartic nonlinear Lakshmanan–Porsezian–Daniel equation in polarization-preserving fibers. *Optik*, 2022, **270**, 170000.
23. Tang, L. Bifurcations and optical solitons for the coupled nonlinear Schrödinger equation in optical fiber Bragg gratings. *J. Opt.*, 2022, **52**, 581–592.
24. Zhou, J., Zhou, R. and Zhu, S. Peakon, rational function and periodic solutions for Tzitzeica–Dodd–Bullough type equations. *Chaos Solitons Fractals*, 2020, **141**, 110419.
25. Xie, Y., Li, L. and Kang, Y. New solitons and conditional stability to the high dispersive nonlinear Schrödinger equation with parabolic law nonlinearity. *Nonlinear Dyn.*, 2021, **103**, 1011–1021.